Obat: Jurnal Riset Ilmu Farmasi dan Kesehatan
Volume. 3 Nomor. 5 September 2025
e-ISSN : 3031-0148, p-ISSN : 3031-013X, Hal. 238-248
DOI: https://doi.org/10.61132/obat.v3i5.1685
Available online at: https://journal.arikesi.or.id/index.php/OBAT

Computational Study of (E)-4-hydroxy-3-(phenylamino)pent-3-en-2-one as A Novel Organic Corrosion Inhibitors

Aseer shakir Ajel
Department of Pathological Analytics Science, College of Applied Medical Science,
Shatrah University, Thi-Qar, 64001, Iraq
Email : aseershakir@shu.edu.iq

Abstract*. This study investigates the corrosion inhibition potential of a newly synthesized organic compound, (E)-4-hydroxy-3-(phenylamino)pent-3-en-2-one (LASA3), using computational chemistry approaches. Density Functional Theory (DFT) calculations were performed at the B3LYP/6-31G(d) level of theory with the Gaussian09 software package to evaluate several key quantum chemical parameters. These parameters include total energy, the energies of the highest occupied molecular orbital (EHOMO) and lowest unoccupied molecular orbital (ELUMO), the energy gap (ΔEgap), dipole moment, chemical hardness, softness (σ), and the number of electrons transferred (ΔN). The computational results reveal that LASA3 exhibits a higher EHOMO value and a smaller ΔEgap compared to its precursor molecules, referred to as S.M.1 and S.M.2. A higher EHOMO value suggests that LASA3 has a greater electron-donating ability, which enhances its interaction with the metal surface. Likewise, the reduced ΔEgap indicates greater chemical reactivity and a higher likelihood of forming stable coordination bonds with iron atoms on the carbon steel surface. Electrostatic potential (ESP) map analysis further supports these findings by highlighting the distribution of electron density within the LASA3 molecule. The ESP maps show significant electron-rich regions localized around nitrogen and oxygen atoms, which are potential active sites for adsorption onto the steel surface. This adsorption process plays a crucial role in blocking active corrosion sites and reducing the rate of metal degradation. In conclusion, the theoretical analysis confirms that LASA3 has superior electronic properties for corrosion inhibition compared to its starting materials, S.M.1 and S.M.2. Its ability to donate electrons, favorable dipole characteristics, and strategically located electron-rich sites make it a promising candidate for further experimental evaluation as an efficient corrosion inhibitor for carbon steel applications.*

Keywords: *Carbon Steel; Computational Study; Corrosion Inhibitor; Enaminone; Β-Dicarbonyl.*

1. INTRODUCTION

Enaminones are class of compounds derived from β-dicarbonyl compound, characterized by a conjugated system involving amine-alkene-carbonyl functional group. Interestingly, these compounds can be categorized into cyclic and acyclic structures, as shown in figure 1.

The enaminone moiety represents an interesting class of organic intermediates that exhibit both nucleophilic and electrophilic reactivity due to their conjugated enamine-carbonyl framework. In addition, enaminones have demonstrated a broad spectrum of biologically activities, such as anti-inflammatory, analgesic, anti-cancer, anti-microbial, anti-depressant and anti-viral.

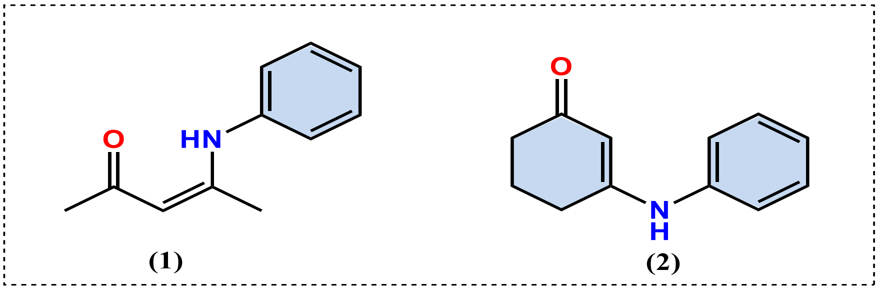

(1)
(2)

Figure 1. Schematic representation for acyclic (1) and cyclic (2) enaminone.

Received: July 05, 2025; Revised: July 20, 2025; Accepted: August 14, 2025; Online Available: August 16, 2025

The corrosion phenomenon that occurs in equipment leads to electrochemical or chemical interactions with the environment. This process can also harm the physical and mechanical properties of equipment, such as oil gas pipes, roads, water and sewage systems and construction, resulting in serious damage and threats to the public safety and health of the community. Some organic compounds were utilized as corrosion inhibitors[8]. Recently, the use of density function theory (DFT) in quantum chemical calculations has been applied to elucidate and establish a connection between experimental results. This approach aims to provide a comprehensive version of the inhibitory effects on metal. Defining the reactivity of a chemical species is highly influenced by the frontier orbital, which comprises the Highest Occupied Molecular Orbital (HOMO) and the Lowest Unoccupied Molecular Orbital (LUMO). The frontier orbital, including HOMO and LUMO of a chemical species, is believed to be very important in defining its reactivity.

2. EXPERIMENTAL SECTION

The novel compound (E)-4-hydroxy-3(phenylamino)pent-3-en-2-one (LASA3) (Figure 2) is synthesized and characterized by mass and FT-IR spectrometers and applied as a corrosion inhibitor on the surface of carbon steel in theoretical calculations.

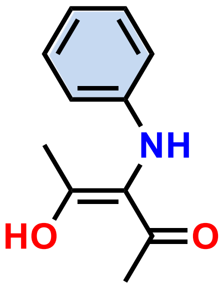

(3)

Figure 2. Schematic representation for (E)-4-hydroxy-3-(phenylamino)pent-3-en-2-one (LASA3).

Materials

Chemicals were sourced commercially and used without further purification. 3-Chloro-2,4-pentanedione, aniline were from BHD. Dimethylformamide, Acetonitrile, Methanol were from Chem-Lab/Belgium. Benzene, Dichloromethane, Hexane, Acetone were from Romil / England. Ethyl acetate was from Scharlau/Eu. Absolute ethanol was from Haymankimia/ England.

Instrumentation

FT-IR spectra are recorded over the spectral range from 400 to 4000 cm-1 for solid sample using SHIMADZU/FT-IR Affinity-1 spectrophotometer and the melting points of the prepared sample was measured using melting point/ SMP3 at Department of Chemistry, College of Science, University of Thi-Qar, Iraq.

Procedure

3-chloro-acetyl acetone (2 ml, 1 eq) dissolved in minimum amount of Dimethylformamide added to a solution of aniline (1 ml, 1 eq) dissolved in minimum amount of Dimethylformamide also. The mixture was heated at 70^{0}C for 25 hours with stirring. [11, 12] The resulting precipitate was collected by filtration, then dried under vacuum to afford the compound LASA3 as brown solid, yield (1.9 gm, 77%), m.p.: 250^{0}C. SAN, EI-MS (m/z): 191 [M]$^{\bullet+}$, 175 [C10H10NO2]$^{\bullet+}$, 159 [C9H7NO2]$^{\bullet+2}$, 149 [C9H9NO]$^{\bullet+}$, 135 [C9H13N]$^{\bullet+}$, 120 [C8H11N]$^{\bullet+}$, 109 [C7H9N]$^{\bullet+}$, 104 [C5H12O2]$^{\bullet+2}$, 93 [C6H7N]$^{\bullet+}$, 88 [C6H7N]$^{\bullet+}$, 77 [C6H5]$^{\bullet+}$, 65 [C5H5]$^{\bullet+}$, 51 [C4H3]$^{\bullet+}$. FT-IR, υ (cm^{-1}): 3367.25 (υO-H) , 3216.19 (υN-H), 3053.11 (υC-H of aromatic), 2921.68 (aliphatic υC-H), 2858.60 (aliphatic υC-H), 1595.24 (υ coupled with υ), 1499.29 (aliphatic C-H bending), 758 and 6697.56 (bending of aromatic C-H). [13-21]

Sub procedure

The calculations were conducted using Density Functional Theory, specifically the B3LYP method, with the 6-31G(d) basis set, using the Gaussian09 program. These calculations aimed to determine the total energy and different electronic properties of the molecules, such as dipole moment, energy of highest occupied molecular orbital (EHOMO), and energy of lowest unoccupied molecular orbital (ELUMO). The purpose of using computational chemistry was to calculate the theoretical results for the corrosion of carbon steel and to define their convergence with the experimental results. A DELL laptop computer with an Intel(R) Core (TM) i7-3820QM CPU 2.70 GHz, 8 GB RAM, and Windows (10) 64-bit operating system was used to calculate the theoretical results for the corrosion of carbon steel.

3. RESULTS AND DISCUSSION

Quantum Chemistry Calculations

Quantum chemistry calculations have proven to be an effective tool for studying the mechanism of corrosion inhibition. Therefore, quantum chemistry calculations are used to obtain information that cannot be obtained from experimental data. One of the most important and prominent molecular properties obtained through computational chemistry calculations is summarized in Table 8, the most important of which are the highest energy occupied molecular orbital (E_{HOMO}), the lowest energy unoccupied molecular orbital (E_{LUMO}), electronegativity, softness (σ), chemical hardness, and the number of transferred electrons ΔN (number of transferred electrons), ionization potential, dipole moment, optimized geometrical shapes (HOMO and LUMO) shapes, and surface electrostatic potential (ESP) of the inhibitor molecules. (LASA3) and its starting materials, represented by (S.M.1) and (S.M.2), are shown in Table 1.

HOMO & LOMO

The highest occupied molecular orbital (HOMO) and the lowest unoccupied molecular orbital (LUMO) are widely distributed on both sides of the two studied compounds, which indicates that the (HN-C-) group in the prepared (E)-4-hydroxy-3-(phenylamino) pent-3-en-2-onecompound represented by the inhibitor (LASA3), in addition to other groups such as phenyl rings, which contain nitrogen (N) and (OH) groups, which are also present in the starting materials that make up the inhibitor (LASA3). According to the figures in Table 1, both the inhibitor (LASA 3) and the starting materials that make up it, which are represented by (S.M.1) and (S.M.2) HOMO orbitals, as well as the presence of (LUMO) orbitals, contain some atoms such as nitrogen atoms in the amine group and other groups such as ($R_2C=O$) and (OH) groups, which are considered electron-donating centers and electron-accepting centers, respectively. Both types work as adsorption centers main.

Table 1. Quantitative chemical data values for the inhibitor (LASA3) and its starting materials (S.M.1) (S.M.2), which were measured using the Density Functional Theory method, at the B3LYP level, with the elements of the basis set 6-31G(d), and using the Gaussian 09 program.

Quantum Chemical parameters	**LASA3**	S.M.1	S.M.2
Total Energy(kJ mol^{-1})	**-2114206.63**	**-754930.14**	**-1659336.85**
Dipole Moment(Debyes)	**2.1891**	**1.9133**	**4.9584**
E_{HOMO}(eV)	**-7.3289**	**-5.1541**	**5.1218**
E_{LUMO}(eV)	**-2.502**	**0.3769**	**-1.252**
$\Delta E_{gap} = E_{LUMO} - E_{HOMO}$(eV)	**4.8265**	**5.531**	**3.8695**
Ionisation potential, $I = -E_{HOMO}$	**7.3289**	**5.1541**	**5.1218**
Electron affinity, $A = -E_{LUMO}$	**2.50238**	**-0.3769**	**1.25228**
Electronegativity (χ), $-\frac{1}{2}(E_{HOMO} + E_{LUMO})$	**4.9156**	**2.3886**	**3.187**

Chemical hardness (η), $\Delta E_{gap}/2$	**2.4133**	**2.7655**	**1.9347**
Softness (σ), $1/\eta$	**0.4144**	**0.3616**	**0.5169**
Chemical Potential $\mu = -1/2(I + A)$	**-4.916**	**-2.389**	**-3.187**
Number of transferred electrons $\Delta N = \chi_{Fe} - \chi_{inh} / [2(\eta_{Fe} + \eta_{inh})]$	**0.43186**	**0.83373**	**0.9854**

The adsorption of the inhibitor to the metal surface occurs on the basis of donor-acceptor interactions between the lone pairs present on the atoms (N and O) present in the structure of the inhibitor (LASA3) and its constituent raw materials, which are represented by (S.M.1 and S.M.2) and the vacant orbitals of the iron atom, in which the boundary orbitals (HOMO and LUMO) of chemical species play a vital role in determining their absorption and interaction. The greater the energy of the higher occupied molecular orbital (E_{HOMO}) is, the greater its tendency to donate electrons to appropriate recipient molecules with empty molecular orbitals. Low energy increases the damping efficiency. Additionally, the lower the energy of the unoccupied molecular orbital (E_{LUMO}), which causes the prepared compound molecule to receive electrons, the greater the inhibition efficiency among the molecules of the compound and its complex, as the inhibitor molecule (LASA3) has the highest energy value of the highest occupied molecular orbital (E_{HOMO}) of (-5.8636 eV) compared to the molecules of its constituent raw materials, represented by (S.M.1 and S.M.2), which have energies (E_{HOMO}) of (-5.7093 and -5.7253 eV) respectively. Therefore, the inhibitor molecule (LASA3) is an easy donor of electrons. This enhances its inhibitory effectiveness compared to the raw materials that make it up.

Energy Gap (ΔE_{gab})

It is also possible to determine the value of the so-called energy gap (ΔE_{gap}), which represents the difference between (E_{HOMO}) and (E_{LUMO}) the inhibitor (Ja) and its constituent raw materials according to the frontier molecular orbital (F_{MO}) theory of chemical reaction; the smaller the orbital energy gap is. ΔEgap had a stronger inhibitory interaction on the steel surface and thus an increase in the inhibition efficiency, as (ΔEgap) had values of (5.685 and 3.310) and (5.033) for both the inhibitor (LASA3) and its constituent raw materials S.M.1 and S.M.2, respectively.

According to the theory of hard and soft acids and bases (HSAB), hard acids tend to react with hard bases, and soft acids react with soft bases. According to this theory, when iron is considered a soft acid, it tends to react more with the inhibitor molecule (LASA3), which can be considered a soft base because it has a low hardness (η) of 1.6547 eV and a high softness (σ) of (0.6043 eV). Therefore, the inhibitor (LASA3) shows better inhibition efficiency than its constituent raw materials, which are represented by (S.M.1 and S.M.2), which have hardness (η) values of (2.5167 and 2.8829 eV) respectively, and a softness (σ) value of (0.3974 and 0.3518 eV) respectively.

The Number of Electrons Transferred (ΔN)

The number of transferred electrons (ΔN) shows the ability of the inhibitor molecule to introduce electrons. The greater the value of (ΔN) is, the greater the ability of the studied inhibitor molecule to introduce electrons to acceptor species that are characterized by electron deficiency (represented in this study by orbitals), d for iron metal surface atoms. In the field of corrosion inhibitors, a high number of transferred electrons (ΔN) indicates there is a great tendency for the studied inhibitor molecule to interact on the metal surface through adsorption processes, which increases inhibition efficiency. According to the observations of Lukovit and others, who assumed that as the number of transferred electrons (ΔN) increases, the electron donation ability of the studied inhibitor molecule to the orbitals of metal surface atoms increases, which leads to an increase in the inhibition efficiency, provided that the number of transferred electrons (ΔN) is < 3.6. ΔN was calculated according to Pearson's theory using equation ($\Delta N = \chi_{Fe} - \chi_{inh}/[2(\eta_{Fe} + \eta_{inh})]$) where χ_{Fe} and χ_{inh} represent the electronegativity of the iron metal and the inhibitor respectively, and ηFe and ηinh represent the chemical hardness (η) of the iron metal and the inhibitor, respectively. The theoretical values for both χ_{Fe} and η_{Fe} are (7.0 and 0 eV.mol-1) respectively, and the values of the number of electrons transferred (ΔN) for both the inhibitor (LASA3) and its starting materials, represented by (S.M.1 and S.M.2) are (0.7242, 0.7564) and (0.8434) respectively.

Surface Electrostatic Potential (ESP)

The study of the surface electrostatic potential (ESP) and the electrostatic potential map of the inhibitor molecule (LASA3) and its constituent raw materials, represented by (S.M.1 and S.M.2), shown in Table 2, is very useful for detecting the locations of the electron density on specific atoms. Therefore, its importance can be included in determining the positive, negative, and neutral electrostatic potential for all atoms of the studied molecule so that we can determine the sites of electrophilic attack that favour the high negativity region (areas of increased electronic density), which are red in colour, while the high positive regions (areas of decreased electronic density), which are blue in color and are preferred sites for nucleophilic attack.

Table 2. Shapes of geometric conformers and molecular orbitals, high and low, electronic density and surface electrostatic potential, quantity of the inhibitor (LASA3) and its starting materials (S.M.1 and S.M.2).

Quantum chemical	LASA3	S.M.1	S.M.2
Structure: Optimized geometry	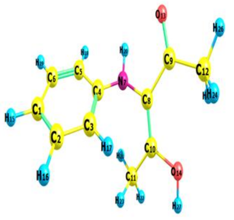	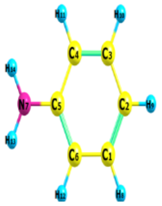	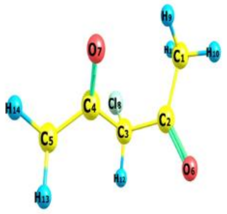
HOMO	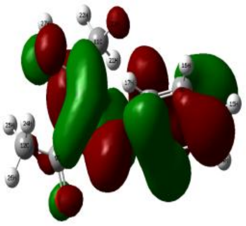	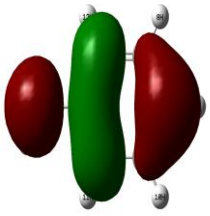	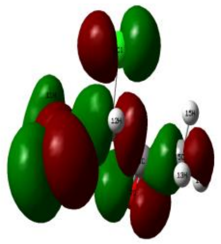
LUMO	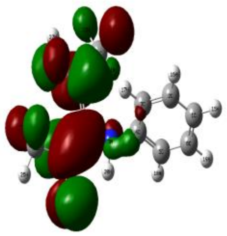	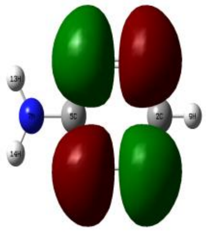	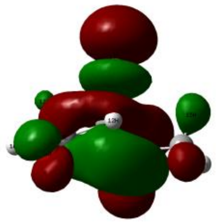
Electrostatic surfaces potential	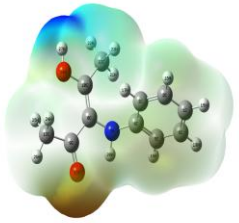	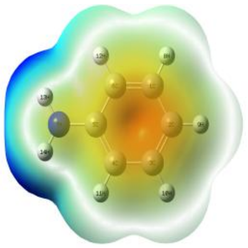	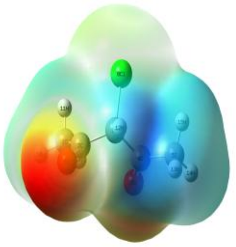

We conclude from the above parameter values that we obtained from the results of computational chemistry that testing the efficiency of inhibition of the inhibitor (LASA3) and its starting materials (S.M.1 and S.M.2) on the iron surface proved that the compound (LASA3) can be considered a better inhibitor. The high values of most of the parameters of the raw materials that make up it, which are represented by (S.M.1 and S.M.2), are comparable to those of the raw materials, especially the number of transferred electrons (ΔN), which means that compound forms a more stable complex on the surface of the metal whose corrosion is to be reduced compared to the raw materials that make it up.

4. CONCLUSION

This investigation employed Density Functional Theory (DFT) to investigate the corrosion inhibition performance of the enaminone compound LASA3 in comparison to its starting materials (S.M.1 and S.M.2) on carbon steel surfaces. Theoretical calculations based on key quantum chemical descriptors—including E_{HOMO}, E_{LUMO}, energy gap (ΔE_{gap}), dipole moment, softness (σ), hardness (η), and number of transferred electrons (ΔN)—revealed that LASA3 exhibits superior electronic properties favoring strong adsorption onto the metal surface.

The lower energy gap (ΔE_{gap} = 4.83 eV), higher E_{HOMO} (-7.33 eV), and significant ΔN value (0.43) for LASA3 indicate enhanced electron-donating ability and strong donor–acceptor interaction with the iron surface. Furthermore, the ESP analysis confirmed the presence of high electron-density regions (on N and O atoms), which serve as primary adsorption centers.

These findings suggest that LASA3 forms a more stable and efficient protective layer on carbon steel than its parent molecules. Thus, LASA3 can be proposed as a promising organic corrosion inhibitor, providing a theoretical foundation for its future application in corrosion prevention strategies.

CONFLICT OF INTEREST

The authors have no conflict of interest.

REFERENCES

Aksh, A. K., Nabi, A. S. A., & Obaid, H. T. (2024). Peganum harmala extract as an eco-friendly corrosion inhibitor for carbon steel N80 in 1 M HCl: Electrochemical and surface morphological studies. *Nanotechnology Perceptions*, 33–49. https://doi.org/10.62441/nano-ntp.v20iS3

Anatheil, A. H., Gatea, A. H., & Neamah, F. O. (2024). Synthesis, characterization, anticorrosion, and computational study of new thiadiazole-oxadiazole derivatives with some transition metal ion. *Journal of Medicinal and Pharmaceutical Chemistry Research*, *6*(8), 1149–1166. https://jmpcr.samipubco.com/article_193247.html

Azhar, H. G. (2018). Synthesis, characterization, antimicrobial of studies new 2,2'-((1Z,2Z)-ethane-1,2-diylidenebis[(2Z)hydrazin-1-yl-2-ylidene-1,3,4-oxadiazole-5,2-diyl])diphenol and their transition metal complexes. *Journal of Global Pharma Technology*, *10*(3), 88–97. http://www.scopus.com/inward/record.url?eid=2-s2.0-85050778444&partnerID=MN8TOARS

Bentiss, F., Lebrini, M., & Lagrenée, M. (2005). Thermodynamic characterization of metal dissolution and inhibitor adsorption processes in mild steel/2,5-bis(n-thienyl)-1,3,4-thiadiazoles/hydrochloric acid system. *Corrosion Science*, *47*(12), 2915–2931. https://doi.org/10.1016/j.corsci.2005.05.034

Chaitra, T. K., Mohana, K. N., & Tandon, H. C. (2017). Comparative study of levofloxacin and its amide derivative as efficient water soluble inhibitors for mild steel corrosion in hydrochloric acid solution. *International Journal of Industrial Chemistry*, *8*(1), 1–15. https://doi.org/10.1007/s40090-016-0083-y

Cleary, T. P., Ji, Y., Lee, G. R., Rawalpally, T., & Sarma, K. (2008). *A novel process for the preparation of 3-amino-pentan-1,5-diol* (Patent No. WO2008151992A2). Google Patents.

Dhaef, H. K., Al-Asadi, R. H., Shenta, A. A., & Mohammed, M. K. (2021). Novel bis maleimide derivatives containing azo group: Synthesis, corrosion inhibition, and theoretical study. *Indonesian Journal of Chemistry*, *21*(5), 1212–1220. https://doi.org/10.22146/ijc.64614

Farghaly, T. A., Alosaimy, A. M., Al-Qurashi, N. T., Masaret, G. S., & Abdulwahab, H. G. (2024). The most recent compilation of reactions of enaminone derivatives with various amine derivatives to generate biologically active compounds. *Mini Reviews in Medicinal Chemistry*, *24*(8), 793–843. https://doi.org/10.2174/1389557523666230913164038

Field, L. D., Sternhell, S., & Kalman, J. R. (2001). Organic structures from spectra. *Angewandte Chemie International Edition, 40*.

Gatea, A. H., Ajel, A. S., & Mhaibes, R. M. (2025). A new method for measuring dopamine in the presence of uric acid employing a carbon paste electrode modified with the UiO-66 metal organic framework-graphene oxide nanocomposite. *ADMET & DMPK*, *13*(2), 2593. https://doi.org/10.5599/admet.2593

Hadi, J. S., Alsalam, B. K., & Essa, A. H. (2009). Synthesis, spectroscopic characterization and theoretical study of Schiff bases derived from phenylsulfonylamide. *Journal of Scientific Research*, *1*, 563–568. https://doi.org/10.3329/jsr.v1i3.2589

Issa, Y. M., Hassib, H. B., & Abdelaal, H. E. (2009). 1H NMR, 13C NMR and mass spectral studies of some Schiff bases derived from 3-amino-1,2,4-triazole. *Spectrochimica Acta Part A: Molecular and Biomolecular Spectroscopy*, *74*, 902–910. https://doi.org/10.1016/j.saa.2009.08.042

Kabanda, M. M., Ebenso, E. E., Murulana, L. C., Kabanda, M. L., & Obi-Egbedi, N. O. (2012). Quantum chemical studies on the corrosion inhibition of mild steel by some triazoles and benzimidazole derivatives in acidic medium. *International Journal of Electrochemical Science*, *7*(6), 5035–5056. https://doi.org/10.1016/S1452-3981(23)19602-7

Kouakou, V., Niamien, P. M., Yapo, A. J., Diaby, S., & Trokourey, A. (2016). Experimental and DFT studies on the behavior of caffeine as effective corrosion inhibitor of copper in 1M HNO3. *Orbital: The Electronic Journal of Chemistry*, *8*(2). https://doi.org/10.17807/orbital.v8i2.804

Kumar, R., Saha, N., Purohit, P., Garg, S. K., Seth, K., Meena, V. S., … Chakraborti, A. K. (2019). Cyclic enaminone as new chemotype for selective cyclooxygenase-2 inhibitory, anti-inflammatory, and analgesic activities. *European Journal of Medicinal Chemistry*, *182*, 111601. https://doi.org/10.1016/j.ejmech.2019.111601

Kumar, R., Saha, N., Purohit, P., Garg, S. K., Seth, K., Meena, V. S., … Chakraborti, A. K. (2019). Cyclic enaminone as new chemotype for selective cyclooxygenase-2 inhibitory, anti-inflammatory, and analgesic activities. *European Journal of Medicinal Chemistry, 182*, 111601. https://doi.org/10.1016/j.ejmech.2019.111601

Li, W., Zhao, X., Liu, F., Deng, J., & Hou, B. (2009). Investigation on the corrosion inhibitive effect of 2H-pyrazole-triazole derivatives in acidic solution. *Materials and Corrosion, 60*(4), 287–293. https://doi.org/10.1002/maco.200805081

Lukovits, I., Kálmán, E., & Zucchi, F. (2001). Corrosion inhibitors – Correlation between electronic structure and efficiency. *Corrosion, 57*(1), 3–8. https://doi.org/10.5006/1.3290328

Madkour, L., & Elroby, S. K. (2015). Inhibitive properties, thermodynamic, kinetics and quantum chemical calculations of polydentate Schiff base compounds as corrosion inhibitors for iron in acidic and alkaline media. *International Journal of Industrial Chemistry, 6*, 165–184. https://doi.org/10.1007/s40090-015-0039-7

Madruga, C., Filho, P. A., Andrade, M. M., Gonçalves, M., Raposo, M., & Ribeiro, P. A. (2011). Birefringence dynamics of poly{1-[4-(3-carboxy-4-hydroxyphenylazo) benzenesulfonamido]-1,2-ethanediyl, sodium salt} cast films. *Thin Solid Films, 519*, 8191–8196. https://doi.org/10.1016/j.tsf.2011.06.102

Mahdi, H. S., Hameed, A., Mohammed, A., & Jassem, I. A. (2022). New benzohydrazide Schiff base: Synthesis, characterization and biological studies. *International Journal of Drug Delivery Technology*. https://doi.org/10.25258/ijddt.12.2.33

Meften, M. J., Radhi, W. A., & Abulhail, A. N. (2018). Molecular structure and electronic characteristics study of imidazole and dioxol derivatives as corrosion inhibitors: A quantum methodology investigation. *Basrah Journal of Science (C), 36*(1), 1–29. https://doi.org/10.29072/basjs.2018302

Obaid, H. T., Kadhum, M. Y., & Abdulnabi, A. S. (2022). Azo Schiff base derived from 2-hydroxy-1-naphthaldehyde as corrosion inhibitors for carbon steel in HCl medium: Experimental and theoretical studies. *Materials Today: Proceedings, 60*, 1394–1401. https://doi.org/10.1016/j.matpr.2021.10.380

Obaid, H. T., Mutar, M. M., & Ali, S. H. (2025). Sulfasalazine as a corrosion inhibitor on carbon steel metal surfaces in acidic media using the hydrogen evolution method: Experimental and theoretical studies. *Indonesian Journal of Chemistry, 25*(1), 90–99. https://doi.org/10.22146/ijc.95852

Oztemel, F., & Berber, I. (2014). Synthesis and biological evaluation of a novel ONS tridentate Schiff base bearing pyrimidine ring and some metal complexes. *Medicinal Chemistry Research, 23*, 3451–3457. https://doi.org/10.1007/s00044-014-0925-0

Pavia, D. L. (2013). *Introduction to spectroscopy* (5th ed.). Cengage Learning.

Pearson, R. G. (1988). Absolute electronegativity and hardness: Application to inorganic chemistry. *Inorganic Chemistry, 27*(4), 734–740. https://doi.org/10.1021/ic00277a030

Sharma, Y. R. (2013). *Elementary organic spectroscopy* (5th ed.). New Age International.

Skoptsova, A. A., Shestakov, A. S., Ledenyova, I. V., Stolpovskaya, N. V., Podoplelova, N. A., Panteleev, M. A., … Novichikhina, N. P. (2022). Reaction of 1-phenacylidene pyrrolo [3,2,1-ij] quinolin-2-ones with cyclic/acyclic enaminones and the anticoagulant activity of synthesized pyrrole-quinoline derivatives. *ChemistrySelect, 7*(46), e202200730. https://doi.org/10.1002/slct.202200730

Thamer, H., Kadhum, M. Y., & Sultan, A. (2022). Quantum chemical calculations and experimental studies of using azo dye as corrosion inhibitors for carbon steel in acidic medium. *[Journal name not provided]*, 2(December), 1–9.

Van, E. S., & Bramer, W. (1998). An introduction to mass spectrometry. Widener University Department of Chemistry.

Xia, S., Qiu, M., Yu, L., Liu, F., & Zhao, H. (2008). Molecular dynamics and density functional theory study on relationship between structure of imidazoline derivatives and inhibition performance. *Corrosion Science, 50*(7), 2021–2029. https://doi.org/10.1016/j.corsci.2008.04.021

Zhao, P., Liang, Q., & Li, Y. (2005). Electrochemical, SEM/EDS and quantum chemical study of phthalocyanines as corrosion inhibitors for mild steel in 1 mol/l HCl. *Applied Surface Science, 252*(5), 1596–1607. https://doi.org/10.1016/j.apsusc.2005.02.121

Zhuo, J. C. (1997). NMR of enaminones part 3 – 1H, 13C and 17O NMR spectroscopic studies of acyclic and cyclic N-aryl enaminones: Substituent effects and intramolecular hydrogen bonding. *Magnetic Resonance in Chemistry, 35*(5), 311–322. https://doi.org/10.1002/(SICI)1097-458X(199705)35:5%3C311::AID-OMR94%3E3.0.CO;2-M